NANO LETTERS

pubs.acs.org/NanoLett Letter

Peptide-Functionalized Lipid Nanoparticles for Targeted Systemic mRNA Delivery to the Brain

Emily L. Han, Sophia Tang, Dongyoon Kim, Amanda M. Murray, Kelsey L. Swingle, Alex G. Hamilton, Kaitlin Mrksich, Marshall S. Padilla, Rohan Palanki, Jacqueline J. Li, and Michael J. Mitchell*

Cite This: *Nano Lett.* 2025, 25, 800−810 Read Online

ACCESS | Metrics & More | Article Recommendations | Supporting Information

ABSTRACT: Systemic delivery of large nucleic acids, such as mRNA, to the brain remains challenging in part due to the blood-brain barrier (BBB) and the tendency of delivery vehicles to accumulate in the liver. Here, we design a peptide-functionalized lipid nanoparticle (LNP) platform for targeted mRNA delivery to the brain. We utilize click chemistry to functionalize LNPs with peptides that target receptors overexpressed on brain endothelial cells and neurons, namely the RVG29, T7, AP2, and mApoE peptides. We evaluate the effect of LNP targeting on brain endothelial and neuronal cell transfection *in vitro*, investigating factors such as serum protein adsorption, intracellular trafficking, endothelial transcytosis, and exosome secretion. Finally, we show that LNP peptide functionalization enhances mRNA transfection in the mouse brain and reduces hepatic delivery after systemic administration. Specifically, RVG29 LNPs improved neuronal transfection *in vivo*, establishing its potential as a nonviral platform for delivering mRNA to the brain.

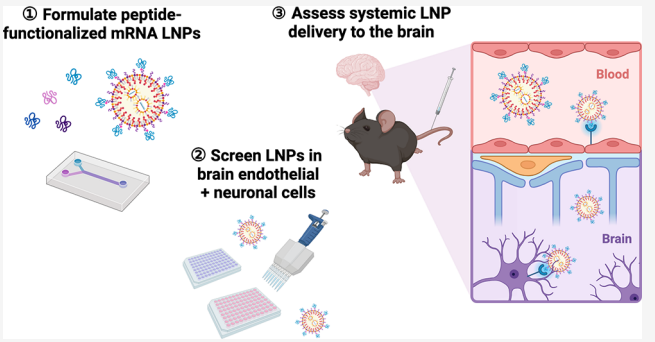

KEYWORDS: *lipid nanoparticles, mRNA, peptides, brain delivery, blood-brain barrier, neurons*

Delivering nucleic acid therapeutics to the brain remains a significant challenge, in part due to the blood-brain barrier (BBB). The BBB prevents ∼98% of small molecule drugs and ∼100% of large molecule drugs, including naked messenger RNA (mRNA), from entering the brain.[1,2] Ionizable lipid nanoparticles (LNPs) have emerged as the most clinically advanced nucleic acid delivery vehicle following the FDA approval of Onpattro and the COVID-19 vaccines.[3,4] However, for applications beyond liver-based therapies and vaccines, achieving tissue-specific delivery has proved difficult with LNPs, motivating groups including ours to explore active targeting strategies. Examples of active targeting strategies for tissue- or cell-specific LNP delivery include functionalization with antibodies targeting the lungs,[5,6] T cells,[7−9] hematopoietic stem cells,[10,11] bone marrow in multiple myeloma,[12] cancer cells and tumor myeloid cells,[13] the placenta,[14] and inflamed cerebral vasculature.[15]

While antibodies have high binding affinity, they also have limitations including immunogenicity, susceptibility to proteases, large size, difficulty achieving a binding-specific orientation, and high production costs.[16,17] Peptides are alternative targeting ligands that address many of these issues. They are only ∼30 amino acids or less in length, enabling higher functionalization density on the nanoparticle surface for improved binding affinity, and compared to antibodies, have lower immunogenicity and production costs.[17] Recent work has demonstrated the ability of peptides to facilitate targeted mRNA LNP delivery to retinal neurons in mice and nonhuman primates.[18] However, the potential of peptides to target LNPs to other tissues remains unexplored.

Here, we design peptide-functionalized LNPs (pLNPs) for systemic mRNA delivery to the brain, targeting receptors highly expressed on both brain endothelial cells and neurons (Figure 1A). The four selected peptides have improved brain delivery of other nanoparticle systems: RVG29 targeting the nicotinic acetylcholine receptor,[19−23] T7 targeting the transferrin receptor,[24−28] angiopep-2 (AP2) targeting low density lipoprotein receptor-related protein 1 (LRP-1),[29−35] and mApoE targeting low density lipoprotein receptor (LDLR).[36−38] mRNA LNPs were functionalized with these peptides at various surface densities via thiol-maleimide click chemistry and facilitated improved transfection efficiency in cultured brain endothelial and neuronal cells. In a coculture transwell model, pLNPs were able to cross the endothelial monolayer and improve transfection of basolateral neuronal

Received: October 18, 2024
Revised: December 2, 2024
Accepted: December 3, 2024
Published: December 17, 2024

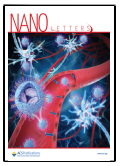

https://doi.org/10.1021/acs.nanolett.4c05186
Nano Lett. 2025, 25, 800−810

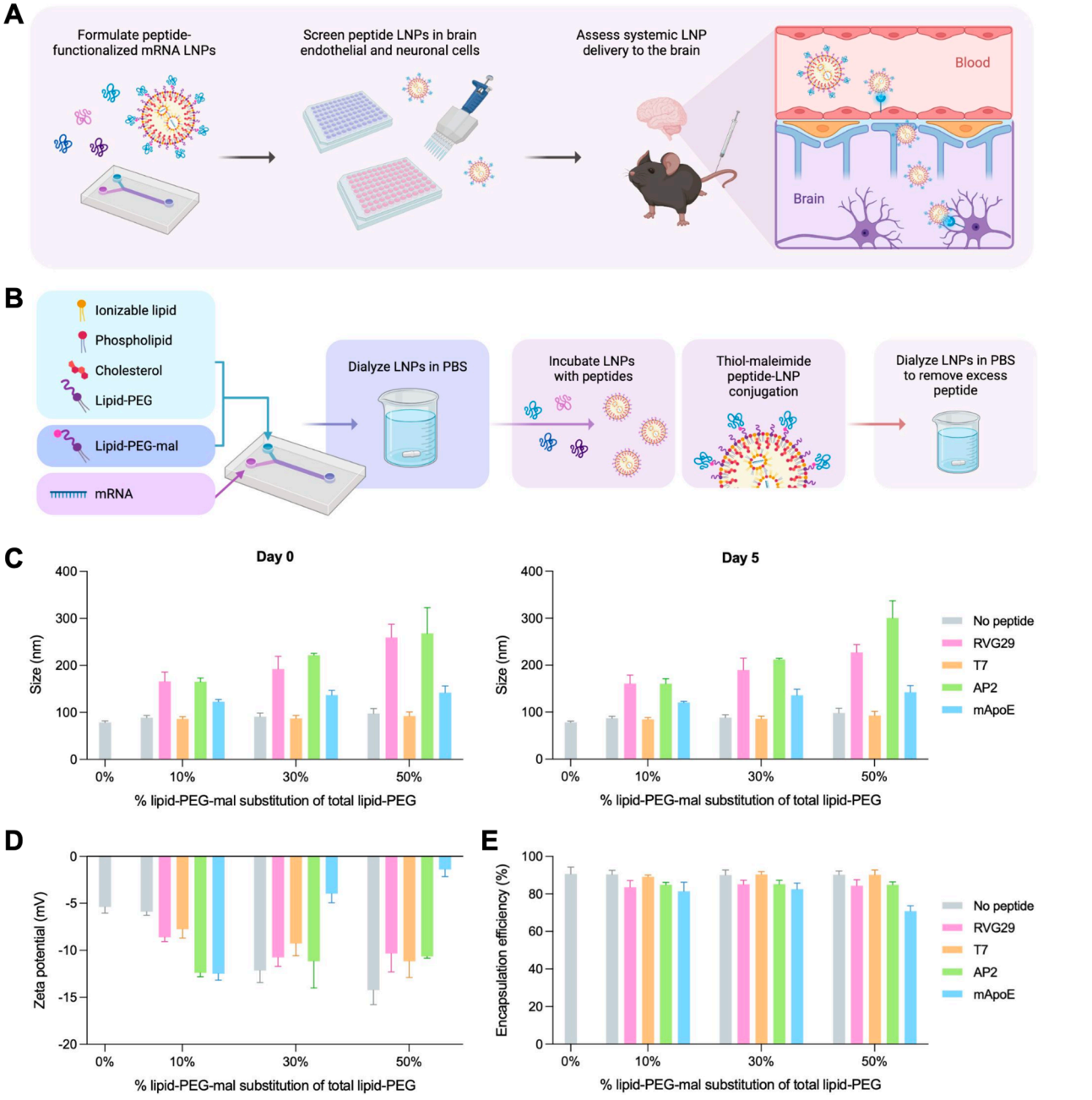

Figure 1. Formulation and characterization of peptide-functionalized LNPs for targeted mRNA delivery to the brain. A) Schematic overview depicting the process of engineering and validating targeted LNPs for brain delivery following systemic administration. Red cells are endothelial cells, orange cells are pericytes, blue cells are astrocytes, and purple cells are neurons. B) Schematic showing the formulation process for targeted LNPs. C) Size of LNPs on days 0 and 5 postformulation. Data are shown as mean + SEM, $n = 2$ formulation replicates each with $n = 3$ technical replicates. D) Zeta potential of LNPs. Data are shown as mean + SEM, $n = 2$ formulation replicates each with $n = 3$ technical replicates. E) mRNA encapsulation efficiency of LNPs. Data are shown as mean + SEM, $n = 2$ formulation replicates.

cells. We also show that exosomes secreted by pLNP-treated brain endothelial cells can transfect neuronal cells. Finally, we demonstrate that pLNPs can transfect the mouse brain after systemic administration, and that specifically RVG29 LNPs significantly improve neuronal transfection compared to untargeted LNPs. Overall, our results demonstrate the promise of pLNPs as a platform for delivering mRNA therapeutics across the BBB for the treatment of various neurological disorders.

Functionalizing mRNA LNPs with Brain-Targeting Peptides. We first sought to determine if the RVG29, T7, AP2, and mApoE peptides could be stably conjugated to mRNA LNPs. For our untargeted LNP, we selected the SM-102 formulation, which has demonstrated clinical success in Moderna's COVID-19 mRNA vaccine with intramuscular administration[39] and was previously shown to enable moderate brain transfection after systemic administration.[40] To formulate pLNPs, we incorporated a fifth lipid component, DSPE-PEG-maleimide (lipid-PEG-mal), which can bind to a terminal cysteine on our peptide sequences via a thiol-maleimide reaction. Since other groups have shown that the surface density of targeting ligands affects delivery across the

https://doi.org/10.1021/acs.nanolett.4c05186
Nano Lett. 2025, 25, 800−810

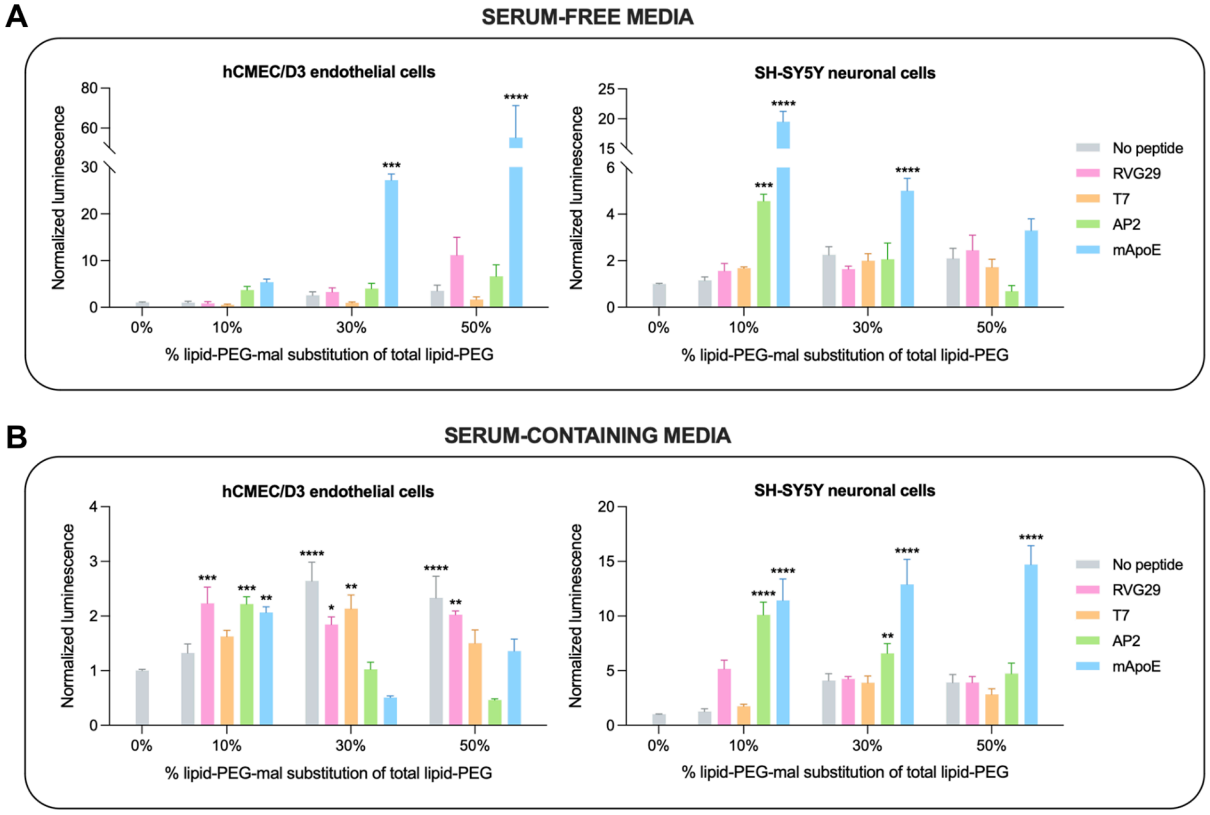

Figure 2. *In vitro* transfection efficacy of peptide-functionalized LNPs in brain endothelial and neuronal cells. A) Luciferase expression in LNP-treated brain endothelial and neuronal cells cultured in serum-free media. Cells were treated with LNPs for 24 h at 60 ng mRNA/20k cells. Data are shown as mean + SEM, $n = 2$ biological replicates each with $n = 4$ technical replicates. B) Luciferase expression in LNP-treated brain endothelial and neuronal cells cultured in 10% FBS-supplemented media. Cells were treated with LNPs for 24 h at 60 ng mRNA/20k cells. Data are shown as mean + SEM, $n = 3$ biological replicates each with $n = 4$ technical replicates. All data are normalized to the untargeted 0% lipid-PEG-mal substitution group. One-way ANOVA with Dunnett's multiple comparisons test was used to determine statistical significance compared to the 0% lipid-PEG-mal substitution group, $*p < 0.05$, $**p < 0.01$, $***p < 0.001$, $****p < 0.0001$.

BBB *in vitro* and *in vivo*,[36,41] we formulated pLNPs with varying amounts of lipid-PEG-mal, substituting it for 10%, 30%, or 50% of the original 1.5 mol % lipid-PEG (Table S1).

LNPs were formulated with luciferase mRNA via microfluidic mixing, then incubated with peptides postformulation for click chemistry-mediated conjugation (Figure 1B). Overall, higher lipid-PEG-mal substitutions led to larger increases in LNP size postconjugation with targeting peptides (Figure 1C). Functionalization with RVG29 and AP2 resulted in the largest increase in size compared to untargeted controls, while T7 led to the smallest increase, highlighting a positive correlation between peptide size and pLNP size. The sizes of all pLNPs were stable 5 days postformulation (Figure 1C). Untargeted LNPs were monodisperse with a polydispersity index (PDI) of ∼0.1, which was maintained for T7 LNPs at all substitutions (Figure S1). RVG29 and mApoE LNPs had PDIs of ∼0.2−0.3, while AP2 LNPs were more polydisperse with PDIs of ∼0.3−0.4. We also assessed the zeta potential of pLNPs to investigate changes in surface charge following peptide functionalization (Figure 1D). Notably, LNPs became less anionic with higher amounts of mApoE. This is likely due to the abundance of lysine and arginine in the mApoE sequence, both of which bear positive charges at neutral pH.

We also confirmed peptide conjugation using two fluorometric protein quantification kits. The FluoProdige kit uses a reagent which binds to lysine, arginine, and histidine. While this kit was able to show the relative difference in peptide concentration pre- and postpurification of excess peptides, the high base fluorescence from the untargeted LNP made interpretation of the peptide concentrations difficult (Figure S2A). This problem was circumvented with the CBQCA kit, which uses a reagent that binds to primary amines and is optimized for protein detection in the presence of lipids and detergents. Using this kit, the untargeted LNP exhibited very low base fluorescence, and the pLNPs displayed peptide concentration values which more closely aligned with their expected yield (Figure S2B). Overall, both kits demonstrate that purification reduces the peptide concentration by approximately half, which was expected given the conjugation reaction was set up at a 2:1 molar ratio of peptide:lipid-PEG-mal and suggests that most of the lipid-PEG-mal molecules are functionalized with peptide. Finally, we confirmed that all pLNPs maintained high mRNA encapsulation efficiencies (Figure 1E) and were not cytotoxic to hCMEC/D3 brain endothelial or SH-SY5Y neuronal cells (Figure S3).

Peptide Targeting Improves mRNA Transfection of Brain Endothelial and Neuronal Cells. We then assessed the potential of peptide functionalization to improve LNP-mediated luciferase mRNA transfection *in vitro*. We began by evaluating transfection efficiency in serum-free media (Figure 2A). In brain endothelial cells, mApoE improved transfection at all lipid-PEG-mal substitutions compared to untargeted 0% substitution LNPs, with 50% substitution mediating a significant ∼60-fold improvement. RVG29 and AP2 at 50%

https://doi.org/10.1021/acs.nanolett.4c05186
Nano Lett. 2025, 25, 800−810

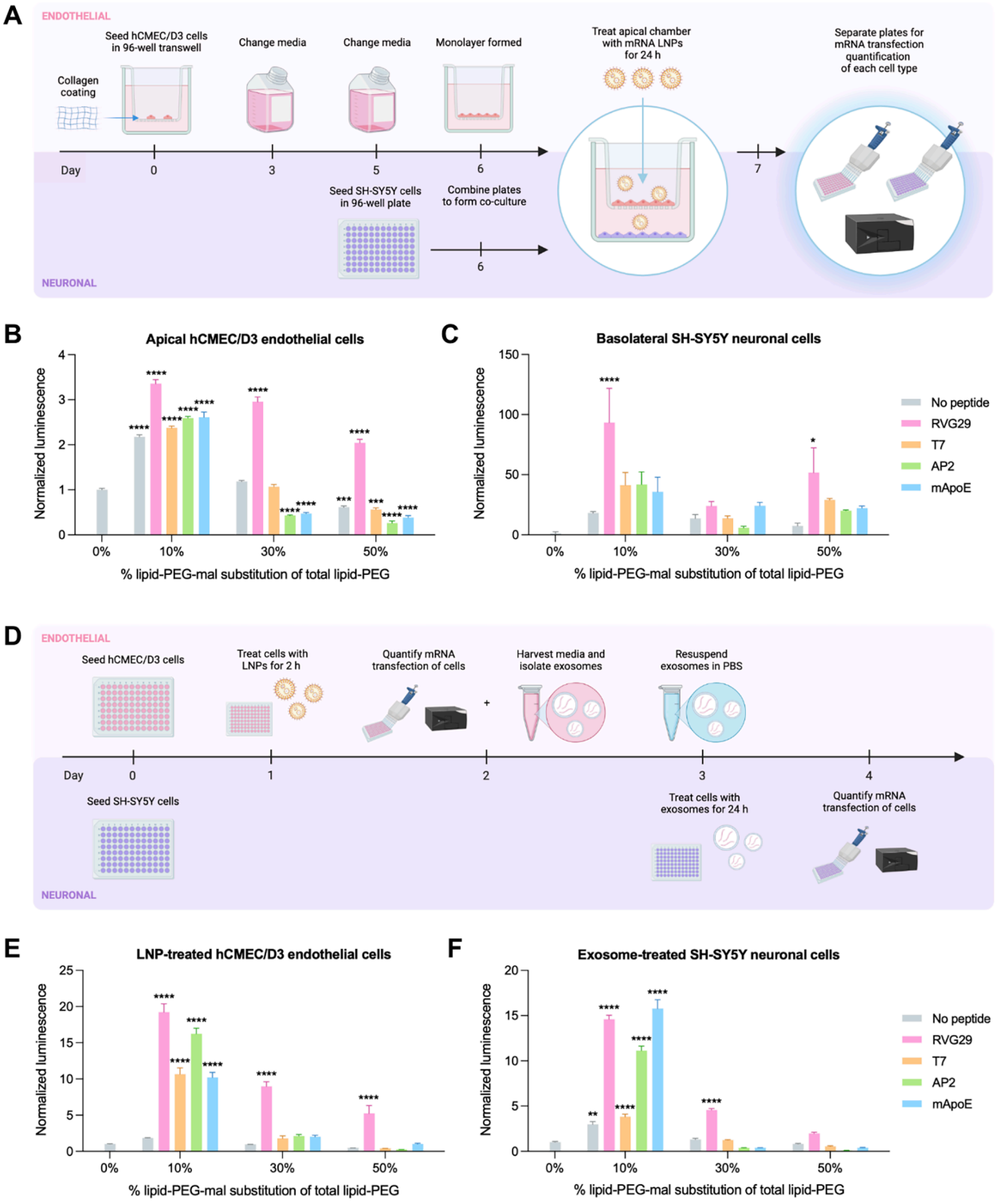

Figure 3. Peptide-functionalized LNP transfection in a BBB transwell and exosome secretion model. A) Schematic depicting the experimental approach for establishing the transwell model. B) Luciferase expression in apical brain endothelial cells treated with LNPs for 24 h at 60 ng mRNA/20k endothelial cells. C) Luciferase expression in basolateral neuronal cells after 24 h. Data are shown as mean + SEM, $n = 3$ technical replicates. D) Schematic depicting the experimental procedure for evaluating the potential of endothelial cell-secreted exosomes to transfect neuronal cells. E) Luciferase expression in brain endothelial cells treated with LNPs for 2 h at 60 ng mRNA/20k cells. F) Luciferase expression in neuronal cells treated with endothelial cell-derived exosomes for 24 h. Data are shown as mean + SEM, $n = 4$ technical replicates. All data are normalized to the untargeted 0% lipid-PEG-mal substitution group. One-way ANOVA with Dunnett's multiple comparisons test was used to determine statistical significance compared to the 0% lipid-PEG-mal substitution group, $*p < 0.05$, $**p < 0.01$, $***p < 0.001$, $****p < 0.0001$.

substitution also improved transfection, whereas T7 showed no improvement at all substitutions tested. In neuronal cells, mApoE LNPs were again the top performing formulations, improving transfection at all substitutions compared to 0%

https://doi.org/10.1021/acs.nanolett.4c05186
Nano Lett. 2025, 25, 800−810

untargeted controls, with 10% substitution mediating a significant ∼20-fold improvement. AP2 at 10% substitution improved transfection by ∼5-fold.

While the serum-free media condition was helpful in assessing the efficacy of peptide targeting, it does not account for the protein corona that forms around nanoparticles under physiological conditions,[42,43] which may interfere with targeting ligands binding to their receptors.[44,45] Thus, we repeated the transfection assays in media supplemented with 10% fetal bovine serum (FBS) (Figure 2B). In brain endothelial cells, the substantial mApoE-induced improvement in transfection over untargeted LNPs detected in the serum-free conditions was no longer observed. Rather, LNPs with 30% and 50% lipid-PEG-mal substitutions without peptides exhibited a significant transfection increase compared to 0% substitution LNPs. The free maleimide groups on these LNPs may be reacting with free thiols on serum proteins, leading to improved cellular uptake. In neuronal cells, mApoE LNPs appeared less susceptible to serum-induced changes in transfection, with all substitutions mediating significant ∼10- to 15-fold improvements compared to 0% substitution LNPs. Interestingly, AP2 LNPs in serum-containing media facilitated greater transfection improvements over untargeted LNPs compared to serum-free media, with all substitutions mediating ∼5- to 10-fold improvements compared to 0% substitution LNPs. Similarly, RVG29 LNPs also facilitated greater transfection improvements over untargeted LNPs in serum-containing media, with all substitutions mediating ∼5-fold improvements.

We also assessed whether these trends would hold in more physiologically relevant conditions by incubating LNPs in 40% human serum prior to treatment (Figure S4). In brain endothelial cells, RVG29 and mApoE LNPs at 10% lipid-PEG-mal substitution retained their transfection efficiency compared to untargeted 0% substitution LNPs, and all 3 formulations demonstrated slightly improved transfection over untargeted LNPs without human serum incubation. In neuronal cells, AP2 and mApoE LNPs at 10% substitution maintained a ∼6-fold improvement compared to 0% substitution LNPs with and without human serum incubation. Overall, it appears that pLNPs made with 10% lipid-PEG-mal substitution are the most resistant to human serum protein adsorption.

Altogether, these data suggest that LNP targeting advantages conferred by peptide functionalization are sensitive to serum protein adsorption. Accordingly, we used serum-containing media for the remainder of our *in vitro* assays to more accurately account for the adsorption of serum proteins. Serum-containing media was also used to confirm that pLNP transfection is dose-dependent (Figure S5), and that top-performing pLNPs for each cell line can also deliver mCherry mRNA, as visualized with fluorescence microscopy (Figure S6, S7). Future work should entail detailed characterization of pLNP protein coronas, both before and after BBB transcytosis, as it has been demonstrated that the corona compositions of other nanoparticles change during BBB transcytosis.[44,46]

Peptide LNPs Enhance BBB Transcytosis and Subsequent Neuronal Transfection *In Vitro*. We next sought to characterize the effect of peptide functionalization on BBB transcytosis. We used a 96-well transwell model that our group has previously established, composed of a brain endothelial monolayer on the transwell insert and neuronal cells in the basolateral compartment, and assessed transfection of both cell types (Figure 3A).[40] In the apical endothelial cells, pLNPs with 10% lipid-PEG-mal substitution demonstrated the highest transfection, each facilitating a significant increase in luciferase expression compared to 0% substitution LNPs (Figure 3B). In the 30% and 50% substitution groups, RVG29 LNPs also demonstrated significant increases in transfection compared to 0% substitution LNPs. In basolateral neuronal cells, similar trends were observed, with targeted 10% substitution LNPs mediating the greatest improvement in transfection compared to 0% substitution LNPs, and RVG29 LNPs bearing significant improvements at 10% and 50% substitution (Figure 3C). Overall, this data shows that while some pLNPs transfect endothelial cells after endocytosis, others are able to transcytose and transfect neuronal cells. The benefit of peptide targeting is most clear in this transwell model, where 10% substitution RVG29 LNPs mediate an almost 100-fold improvement in neuronal transfection post-BBB crossing.

Next, we further investigated the mechanisms of LNP endocytosis and transcytosis. We first used fluorescence microscopy to track the intracellular distribution of pLNPs in brain endothelial cells over the course of 24 h. Cells were treated with luciferase mRNA LNPs labeled with fluorescent dye DiR for 2 h, and then, after a total of 2, 4, 12, or 24 h of incubation, stained with LysoTracker to visualize acidic compartments such as late endosomes and lysosomes (Figure S8). Yellow signal indicates colocalization of red DiR and green LysoTracker. Cells treated with untargeted LNPs demonstrated low DiR and yellow signal at 2 h, indicating limited LNP uptake. Cells treated with RVG29 LNPs had more yellow signal at 2 h, indicating higher LNP uptake and endosome acidification, as well as diffuse DiR signal at 24 h, indicating endosomal escape. T7 and mApoE LNPs demonstrated the highest cellular uptake with bright DiR signal at 12 and 24 h, however the LysoTracker signal was lower than that of RVG29 at 2 h, potentially indicating that the high LNP accumulation inhibited the endosomal acidification necessary for mRNA release and expression.[47] Overall, these results could explain why the 10% substitution RVG29 LNPs facilitated the highest basolateral neuronal transfection in the transwell study—these LNPs may enable higher cellular uptake combined with efficient endosome acidification, which allows increased cargo release for both transfection and basolateral secretion.

To further investigate this hypothesis, we conducted experiments to study how peptide functionalization affects the endothelial secretion of LNPs and mRNA cargo. Recent literature has suggested that after LNP endocytosis, mRNA cargo is repackaged and secreted in extracellular vesicles, which then mediate gene transfer to other cells.[48−50] We hypothesized that a similar mechanism may occur when LNPs cross the BBB and sought to evaluate this in a proof-of-concept experiment where exosomes were isolated from pLNP-treated endothelial cells (Figure 3D). In this model, the observed endothelial transfection trends were similar to those from the transwell study, with 10% lipid-PEG-mal substitution pLNPs yielding the highest improvement compared to 0% substitution LNPs, and RVG29 LNPs performing the best across all substitutions (Figure 3E). The higher magnitudes of improvement compared to earlier experiments is likely a result of the shorter treatment period (2 versus 24 h), as receptor-mediated endocytosis may mediate more rapid cellular uptake. For instance, TfR-targeted immunoliposomes had greater improve-

https://doi.org/10.1021/acs.nanolett.4c05186
Nano Lett. 2025, 25, 800−810

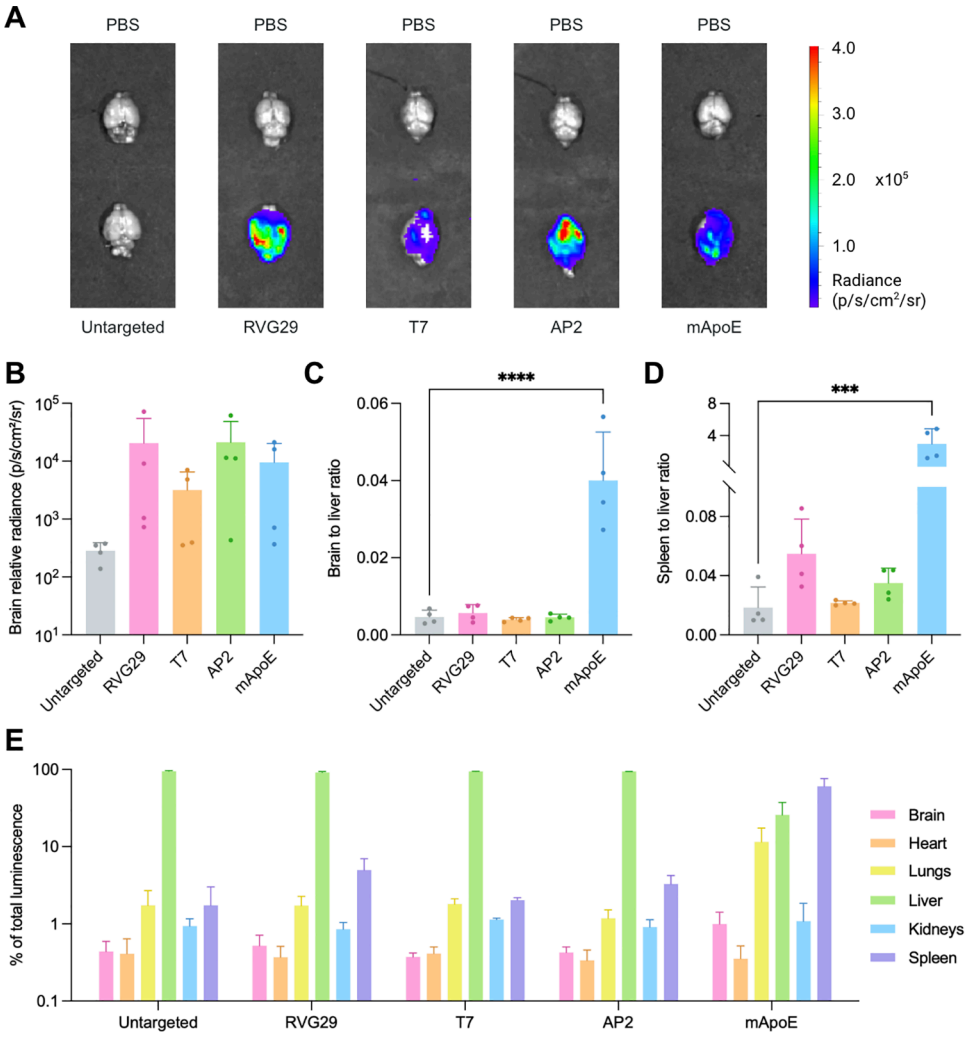

Figure 4. *In vivo* mRNA transfection after intravenous administration of peptide-functionalized LNPs. A) Representative *in vivo* imaging system (IVIS) images and B) quantification of luciferase mRNA transfection in the brain in adult C57BL/6 mice. Untargeted LNPs have 0% lipid-PEG-mal substitution, targeted LNPs have 10% lipid-PEG-mal substitution. Mice were injected intravenously with LNPs at a dose of 0.3 mg/kg mRNA or PBS and sacrificed after 6 h. Representative IVIS images are shown from the mice with the greatest luciferase expression in the brain for each group. Relative radiance was calculated by subtracting PBS group luminescence from LNP groups. C) Brain to liver and D) spleen to liver luminescence ratios for LNP-treated mice. Data are shown as mean + SD with $n = 4$ mice. One-way ANOVA with Dunnett's multiple comparisons test was used to determine statistical significance compared to the 0% substitution group, ***$p < 0.001$, ****$p < 0.0001$. E) Distribution of luminescence across brain, heart, lungs, liver, kidneys, and spleen. Data are shown as % of total luminescence = (organ luminescence)/(total organ luminescence)*100.

ments in brain capillary accumulation over untargeted immunoliposomes at 1 h compared to 24 h.[51]

Neuronal cells treated with the isolated exosomes also demonstrated luminescence, indicating that the isolated exosomes encapsulated luciferase mRNA (Figure 3F). Exosomes derived from 10% substitution pLNP groups significantly improved transfection compared to those from the 0% substitution group. Specifically, exosomes derived from cells treated with RVG29 and mApoE LNPs yielded a ∼15-fold improvement. Future work should investigate whether the LNPs are exocytosed intact, or whether the lipid, mRNA, and peptide components are being repackaged into endogenous exosomes. These studies should also assess whether secretion occurs preferentially at the luminal or abluminal side of endothelial cells and elucidate the biological mechanisms behind these trends.

Peptide LNPs Improve *In Vivo* Brain Transfection after Systemic Administration. We next evaluated whether peptide targeting could improve *in vivo* mRNA transfection in the brain after systemic administration. Based on the *in vitro* screening data, 10% lipid-PEG-mal substitution was selected for all pLNPs. LNPs were formulated with luciferase mRNA and intravenously administered to healthy adult C57BL/6 mice at a dose of 0.3 mg/kg. After 6 h, luciferin was intraperitoneally administered, and mice were euthanized for organ collection and *ex vivo* imaging (Figure S9).

All pLNPs facilitated improvements in brain transfection compared to untargeted LNPs, with RVG29 and AP2 enabling a ∼70-fold improvement (Figure 4A,B). The brain-to-liver ratio for mice treated with mApoE LNPs was ∼8-fold greater than the those treated with untargeted LNPs (Figure 4C). This LNP also outperformed other LNPs in terms of extrahepatic delivery, with increased transfection of the spleen and lungs as well (Figure 4D,E). While for all other LNPs at least 90% of the total organ luminescence originated from the liver, for mApoE LNPs, only 25% of signal originated from the liver

https://doi.org/10.1021/acs.nanolett.4c05186
Nano Lett. 2025, 25, 800−810

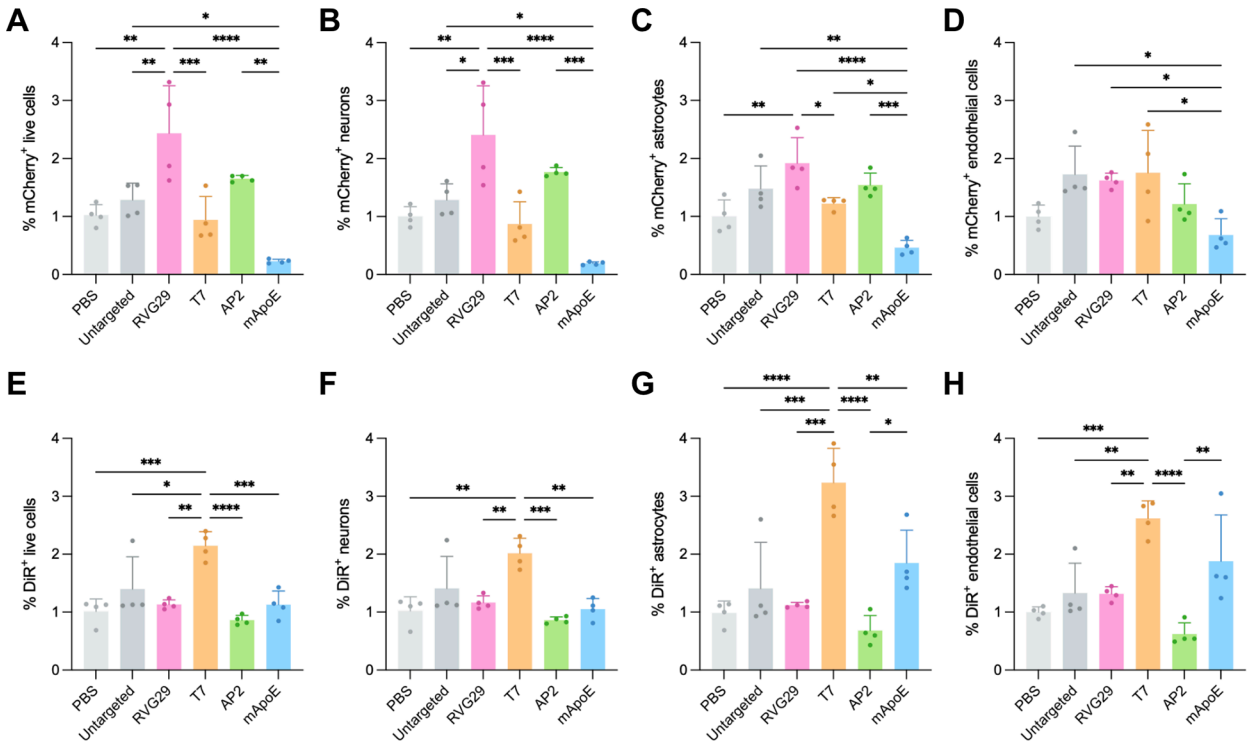

Figure 5. Cell-specific flow cytometric analysis of *in vivo* mRNA LNP transfection and uptake in the brain. The percentage of mCherry$^+$ cells in A) live cells, B) neurons, C) astrocytes, and D) endothelial cells and the percentage of DiR$^+$ cells in E) live cells, F) neurons, G) astrocytes, and H) endothelial cells from adult C57BL/6 mice treated with mCherry mRNA LNPs containing 1 mol % DiR. Untargeted LNPs have 0% lipid-PEG-mal substitution, peptide-functionalized LNPs have 10% lipid-PEG-mal substitution. Mice were injected intravenously with LNPs at a dose of 0.3 mg/kg mRNA or PBS and sacrificed after 12 h. Bar graphs are reported as mean + SD with $n = 4$ mice. One-way ANOVA with Tukey's multiple comparisons test was used to determine statistical significance, *$p < 0.05$, **$p < 0.01$, ***$p < 0.001$, ****$p < 0.0001$.

with the largest contribution being from the spleen (Figure 4E). Indeed, the spleen-to-liver ratio for mice treated with mApoE LNPs was ∼160-fold greater than those treated with untargeted LNPs (Figure 4D). This is an interesting observation considering that serum ApoE has been shown to drive LNP delivery to hepatocytes via LDLR,[52,53] as we observed with untargeted LNPs (Figure 4E). This suggests that though the mApoE sequence is derived from ApoE, the two lead to different LNP organ tropisms; however, the specific mechanisms behind this phenomenon remain unclear. To reduce off target delivery, future work should involve designing peptides that target receptors expressed more exclusively in the brain. High-throughput approaches, such as phage display screening for identifying new peptides and DNA or mRNA barcoding for LNP library screening,[54−57] may be useful in these pursuits.

LNP Peptide Targeting Enhances Transfection of Neurons *In Vivo*. Finally, we investigated cell type-specific transfection and uptake in the brain with our pLNP formulations. LNPs were formulated with mCherry mRNA and 1 mol % DiR and intravenously administered to healthy adult C57BL/6 mice at a dose of 0.3 mg/kg. After 12 h, mice were euthanized, and the brains were processed for flow cytometric analysis. A representative gating strategy is shown in Figure S10.

When evaluating all live cells, RVG29 LNPs mediated a significant increase in the percentage of mCherry$^+$ cells compared to untargeted LNPs (Figure 5A). NeuN$^+$ neurons from mice treated with RVG29 LNPs were ∼2.4% mCherry$^+$, whereas neurons from mice treated with untargeted LNPs were only ∼1.2% mCherry$^+$, which was very close to the background autofluorescence from the PBS-treated group (Figure 5B). GFAP$^+$/CD31$^-$/NeuN$^-$ astrocytes from mice treated with RVG29 LNPs were ∼1.9% mCherry$^+$, whereas astrocytes from mice treated with untargeted LNPs were ∼1.4% mCherry$^+$, though this difference was not statistically significant (Figure 5C). In CD31$^+$/GFAP$^-$/NeuN$^-$ endothelial cells, untargeted, RVG29, and T7 LNPs facilitated similar levels of mCherry transfection (Figure 5D). Notably, though T7 LNP treatment led to the highest percentage of DiR$^+$ live cells, neurons, astrocytes, and endothelial cells compared to other groups (Figure 5E-H), this did not directly correlate to improved transfection. This corroborates what was observed *in vitro*, where T7 and mApoE LNPs exhibited higher endothelial uptake compared to RVG29 LNPs (Figure S8) but not higher transfection (Figures 2B and 3B,E). These findings underscore the importance of screening for both transfection and uptake when delivering nucleic acids like mRNA. Mean fluorescence intensities (MFIs) for flow cytometry data are shown in Figure S11.

Together, this data shows that RVG29 LNPs facilitate significant improvements in transfecting neurons but not endothelial cells, suggesting that these targeted formulations are able to cross the BBB and avoid entrapment in endothelial cells. Notably, the identification of RVG29 LNPs as the top performer for neuronal transfection *in vivo* aligns with the results of the *in vitro* coculture transwell study (Figure 3C), highlighting the utility of this *in vitro* screening platform for predicting *in vivo* results. Future work may entail adding

https://doi.org/10.1021/acs.nanolett.4c05186
Nano Lett. 2025, 25, 800−810

additional cell types of interest to this analysis, such as microglia or oligodendrocytes.

In conclusion, we have designed a peptide-functionalized LNP platform for targeted mRNA delivery to the brain after systemic administration. Through *in vitro* evaluation in endothelial and neuronal cells and *in vivo* studies, we identified an RVG29 LNP formulation with a 10% lipid-PEG-mal substitution that was able to improve neuronal transfection *in vivo* with low entrapment in BBB endothelial cells. Potential limitations of this work include the fact that peptide conjugation increases the size of LNPs, which could hinder diffusion through the extracellular space of the brain and prevent LNPs from reaching deeper areas of parenchyma. Another important consideration for furthering this work is the effect of disease and aging on receptor expression.[58,59] For instance, LRP-1 expression on the BBB has been reported to be downregulated in Alzheimer's disease[58] and aging.[60] Accordingly, targeting peptides should be thoughtfully selected and evaluated for specific therapeutic applications. Overall, our study demonstrates the potential of peptide targeting to improve systemic mRNA delivery to the brain, and the preferential neuronal transfection mediated by RVG29 LNPs suggests its promise as a potential candidate for treating neurological disorders.

■ ASSOCIATED CONTENT

Supporting Information

The Supporting Information is available free of charge at https://pubs.acs.org/doi/10.1021/acs.nanolett.4c05186.

Materials and methods, additional LNP library characterization data, LNP cytotoxicity data, LNP dose response, microscopy images, IVIS organ images and quantification, and additional flow information and data (PDF)

■ AUTHOR INFORMATION

Corresponding Author

Michael J. Mitchell − *Department of Bioengineering, University of Pennsylvania, Philadelphia, Pennsylvania 19104, United States; Institute for Immunology, Perelman School of Medicine, Cardiovascular Institute, Perelman School of Medicine, Abramson Cancer Center, Perelman School of Medicine, and Penn Institute for RNA Innovation, Perelman School of Medicine, University of Pennsylvania, Philadelphia, Pennsylvania 19104, United States; Institute for Regenerative Medicine, Perelman School of Medicine, University of Pennsylvania, Philadelphia, Pennsylvania 19104, United States;* orcid.org/0000-0002-3628-2244; Email: mjmitch@seas.upenn.edu

Authors

Emily L. Han − *Department of Bioengineering, University of Pennsylvania, Philadelphia, Pennsylvania 19104, United States;* orcid.org/0009-0008-6276-7502

Sophia Tang − *Department of Bioengineering, University of Pennsylvania, Philadelphia, Pennsylvania 19104, United States;* orcid.org/0009-0008-2506-682X

Dongyoon Kim − *Department of Bioengineering, University of Pennsylvania, Philadelphia, Pennsylvania 19104, United States;* orcid.org/0000-0002-1769-6505

Amanda M. Murray − *Department of Bioengineering, University of Pennsylvania, Philadelphia, Pennsylvania 19104, United States;* orcid.org/0009-0000-2124-351X

Kelsey L. Swingle − *Department of Bioengineering, University of Pennsylvania, Philadelphia, Pennsylvania 19104, United States;* orcid.org/0000-0001-8475-9206

Alex G. Hamilton − *Department of Bioengineering, University of Pennsylvania, Philadelphia, Pennsylvania 19104, United States;* orcid.org/0000-0002-9810-5630

Kaitlin Mrksich − *Department of Bioengineering, University of Pennsylvania, Philadelphia, Pennsylvania 19104, United States;* orcid.org/0009-0008-7971-2129

Marshall S. Padilla − *Department of Bioengineering, University of Pennsylvania, Philadelphia, Pennsylvania 19104, United States;* orcid.org/0000-0003-3607-790X

Rohan Palanki − *Department of Bioengineering, University of Pennsylvania, Philadelphia, Pennsylvania 19104, United States; Center for Fetal Research, Children's Hospital of Philadelphia, Philadelphia, Pennsylvania 19104, United States;* orcid.org/0000-0001-5168-5634

Jacqueline J. Li − *Department of Bioengineering, University of Pennsylvania, Philadelphia, Pennsylvania 19104, United States;* orcid.org/0000-0002-7849-5483

Complete contact information is available at: https://pubs.acs.org/10.1021/acs.nanolett.4c05186

Author Contributions

E.L.H. and M.J.M. conceived the project and designed the experiments. The experiments were performed by E.L.H., S.T., D.K., A.M.M., K.L.S., A.G.H., K.M., M.S.P., R.P., and J.J.L. and interpreted by all authors. E.L.H. prepared the figures and wrote the manuscript. E.L.H., K.L.S., A.M.M., R.P., and M.J.M. edited and revised the manuscript. All authors reviewed the manuscript and figures and approved the final version for submission.

Funding

M.J.M. acknowledges support from a US National Institutes of Health (NIH) Director's New Innovator Award (DP2 TR002776), a Burroughs Wellcome Fund Career Award at the Scientific Interface (CASI), a US National Science Foundation CAREER Award (CBET-2145491), and an American Cancer Society Research Scholar Grant (RSG-22-122-01-ET). E.L.H., A.M.M., K.L.S., and A.G.H. acknowledge support from an NSF Graduate Research Fellowship (Award 1845298). M.S.P. acknowledges support from the National Institute of Dental and Craniofacial Research of the NIH (T90DE030854). R.P. acknowledges support from an NIH NHLBI F30 fellowship (F30HL162465-01A1).

Notes

The authors declare the following competing financial interest(s): E.L.H. and M.J.M. are inventors on a patent related to this work filed by the Trustees of the University of Pennsylvania (U.S. Provisional Patent Application No. 63/710,179, filed October 22, 2024). All other authors declare they have no competing interests.

■ ACKNOWLEDGMENTS

We would like to thank Dr. Paula Hammond's group for graciously donating hCMEC/D3 cells and Dr. Ian Blair's group for graciously donating SH-SY5Y cells used in this work. Figure schematics were created with BioRender. Data for this manuscript were generated in the University of Pennsylvania's

CDB Microscopy Core. Data were also generated in the Penn Cytomics and Cell Sorting Shared Resource Laboratory at the University of Pennsylvania (RRID:SCR_022376), which was partially supported by the Abramson Cancer Center NCI Grant (P30 016520).

REFERENCES

(1) Pardridge, W. M. The Blood-Brain Barrier: Bottleneck in Brain Drug Development. *NeuroRX* **2005**, *2* (1), 3−14.
(2) Wu, J. R.; Hernandez, Y.; Miyasaki, K. F.; Kwon, E. J. Engineered Nanomaterials That Exploit Blood-Brain Barrier Dysfunction for Delivery to the Brain. *Adv. Drug Delivery Rev.* **2023**, *197*, 114820.
(3) Hou, X.; Zaks, T.; Langer, R.; Dong, Y. Lipid Nanoparticles for mRNA Delivery. *Nat. Rev. Mater.* **2021**, *6* (12), 1078−1094.
(4) Jeong, M.; Lee, Y.; Park, J.; Jung, H.; Lee, H. Lipid Nanoparticles (LNPs) for *in Vivo* RNA Delivery and Their Breakthrough Technology for Future Applications. *Adv. Drug Delivery Rev.* **2023**, *200*, 114990.
(5) Parhiz, H.; Shuvaev, V. V.; Pardi, N.; Khoshnejad, M.; Kiseleva, R. Y.; Brenner, J. S.; Uhler, T.; Tuyishime, S.; Mui, B. L.; Tam, Y. K.; Madden, T. D.; Hope, M. J.; Weissman, D.; Muzykantov, V. R. PECAM-1 Directed Re-Targeting of Exogenous mRNA Providing Two Orders of Magnitude Enhancement of Vascular Delivery and Expression in Lungs Independent of Apolipoprotein E-Mediated Uptake. *J. Control. Release Off. J. Control. Release Soc.* **2018**, *291*, 106−115.
(6) Li, Q.; Chan, C.; Peterson, N.; Hanna, R. N.; Alfaro, A.; Allen, K. L.; Wu, H.; Dall'Acqua, W. F.; Borrok, M. J.; Santos, J. L. Engineering Caveolae-Targeted Lipid Nanoparticles To Deliver mRNA to the Lungs. *ACS Chem. Biol.* **2020**, *15* (4), 830−836.
(7) Tombácz, I.; Laczkó, D.; Shahnawaz, H.; Muramatsu, H.; Natesan, A.; Yadegari, A.; Papp, T. E.; Alameh, M.-G.; Shuvaev, V.; Mui, B. L.; Tam, Y. K.; Muzykantov, V.; Pardi, N.; Weissman, D.; Parhiz, H. Highly Efficient CD4+ T Cell Targeting and Genetic Recombination Using Engineered CD4+ Cell-Homing mRNA-LNPs. *Mol. Ther.* **2021**, *29* (11), 3293−3304.
(8) Rurik, J. G.; Tombácz, I.; Yadegari, A.; Méndez Fernández, P. O.; Shewale, S. V.; Li, L.; Kimura, T.; Soliman, O. Y.; Papp, T. E.; Tam, Y. K.; Mui, B. L.; Albelda, S. M.; Puré, E.; June, C. H.; Aghajanian, H.; Weissman, D.; Parhiz, H.; Epstein, J. A. CAR T Cells Produced in Vivo to Treat Cardiac Injury. *Science* **2022**, *375* (6576), 91−96.
(9) Billingsley, M. M.; Gong, N.; Mukalel, A. J.; Thatte, A. S.; El-Mayta, R.; Patel, S. K.; Metzloff, A. E.; Swingle, K. L.; Han, X.; Xue, L.; Hamilton, A. G.; Safford, H. C.; Alameh, M.-G.; Papp, T. E.; Parhiz, H.; Weissman, D.; Mitchell, M. J. In Vivo mRNA CAR T Cell Engineering via Targeted Ionizable Lipid Nanoparticles with Extrahepatic Tropism. *Small* **2024**, *20* (11), 2304378.
(10) Palanki, R.; Riley, J. S.; Bose, S. K.; Luks, V.; Dave, A.; Kus, N.; White, B. M.; Ricciardi, A. S.; Swingle, K. L.; Xue, L.; Sung, D.; Thatte, A. S.; Safford, H. C.; Chaluvadi, V. S.; Carpenter, M.; Han, E. L.; Maganti, R.; Hamilton, A. G.; Mrksich, K.; Billingsley, M. B.; Zoltick, P. W.; Alameh, M.-G.; Weissman, D.; Mitchell, M. J.; Peranteau, W. H. In Utero Delivery of Targeted Ionizable Lipid Nanoparticles Facilitates in Vivo Gene Editing of Hematopoietic Stem Cells. *Proc. Natl. Acad. Sci. U. S. A.* **2024**, *121* (32), No. e2400783121.
(11) Breda, L.; Papp, T. E.; Triebwasser, M. P.; Yadegari, A.; Fedorky, M. T.; Tanaka, N.; Abdulmalik, O.; Pavani, G.; Wang, Y.; Grupp, S. A.; Chou, S. T.; Ni, H.; Mui, B. L.; Tam, Y. K.; Weissman, D.; Rivella, S.; Parhiz, H. In Vivo Hematopoietic Stem Cell Modification by mRNA Delivery. *Science* **2023**, *381* (6656), 436−443.
(12) Tarab-Ravski, D.; Hazan-Halevy, I.; Goldsmith, M.; Stotsky-Oterin, L.; Breier, D.; Naidu, G. S.; Aitha, A.; Diesendruck, Y.; Ng, B. D.; Barsheshet, H.; Berger, T.; Vaxman, I.; Raanani, P.; Peer, D. Delivery of Therapeutic RNA to the Bone Marrow in Multiple Myeloma Using CD38-Targeted Lipid Nanoparticles. *Adv. Sci.* **2023**, *10* (21), 2301377.
(13) Yong, S.-B.; Ramishetti, S.; Goldsmith, M.; Diesendruck, Y.; Hazan-Halevy, I.; Chatterjee, S.; Somu Naidu, G.; Ezra, A.; Peer, D. Dual-Targeted Lipid Nanotherapeutic Boost for Chemo-Immunotherapy of Cancer. *Adv. Mater.* **2022**, *34* (13), 2106350.
(14) Geisler, H. C.; Ghalsasi, A. A.; Safford, H. C.; Swingle, K. L.; Thatte, A. S.; Mukalel, A. J.; Gong, N.; Hamilton, A. G.; Han, E. L.; Nachod, B. E.; Padilla, M. S.; Mitchell, M. J. EGFR-Targeted Ionizable Lipid Nanoparticles Enhance *in Vivo* mRNA Delivery to the Placenta. *J. Controlled Release* **2024**, *371*, 455−469.
(15) Marcos-Contreras, O. A.; Greineder, C. F.; Kiseleva, R. Y.; Parhiz, H.; Walsh, L. R.; Zuluaga-Ramirez, V.; Myerson, J. W.; Hood, E. D.; Villa, C. H.; Tombacz, I.; Pardi, N.; Seliga, A.; Mui, B. L.; Tam, Y. K.; Glassman, P. M.; Shuvaev, V. V.; Nong, J.; Brenner, J. S.; Khoshnejad, M.; Madden, T.; Weissmann, D.; Persidsky, Y.; Muzykantov, V. R. Selective Targeting of Nanomedicine to Inflamed Cerebral Vasculature to Enhance the Blood-Brain Barrier. *Proc. Natl. Acad. Sci. U. S. A.* **2020**, *117* (7), 3405−3414.
(16) Todaro, B.; Ottalagana, E.; Luin, S.; Santi, M. Targeting Peptides: The New Generation of Targeted Drug Delivery Systems. *Pharmaceutics* **2023**, *15* (6), 1648.
(17) Liu, M.; Fang, X.; Yang, Y.; Wang, C. Peptide-Enabled Targeted Delivery Systems for Therapeutic Applications. *Front. Bioeng. Biotechnol.* **2021**, *9*, 1.
(18) Herrera-Barrera, M.; Ryals, R. C.; Gautam, M.; Jozic, A.; Landry, M.; Korzun, T.; Gupta, M.; Acosta, C.; Stoddard, J.; Reynaga, R.; Tschetter, W.; Jacomino, N.; Taratula, O.; Sun, C.; Lauer, A. K.; Neuringer, M.; Sahay, G. Peptide-Guided Lipid Nanoparticles Deliver mRNA to the Neural Retina of Rodents and Nonhuman Primates. *Sci. Adv.* **2023**, *9* (2), No. eadd4623.
(19) Kumar, P.; Wu, H.; McBride, J. L.; Jung, K.-E.; Hee Kim, M.; Davidson, B. L.; Kyung Lee, S.; Shankar, P.; Manjunath, N. Transvascular Delivery of Small Interfering RNA to the Central Nervous System. *Nature* **2007**, *448* (7149), 39−43.
(20) Liu, Y.; Huang, R.; Han, L.; Ke, W.; Shao, K.; Ye, L.; Lou, J.; Jiang, C. Brain-Targeting Gene Delivery and Cellular Internalization Mechanisms for Modified Rabies Virus Glycoprotein RVG29 Nanoparticles. *Biomaterials* **2009**, *30* (25), 4195−4202.
(21) Han, H.; Zhang, Y.; Jin, S.; Chen, P.; Liu, S.; Xie, Z.; Jing, X.; Wang, Z. Paclitaxel-Loaded Dextran Nanoparticles Decorated with RVG29 Peptide for Targeted Chemotherapy of Glioma: An in Vivo Study. *New J. Chem.* **2020**, *44* (15), 5692−5701.
(22) Pinheiro, R. G. R.; Granja, A.; Loureiro, J. A.; Pereira, M. C.; Pinheiro, M.; Neves, A. R.; Reis, S. RVG29-Functionalized Lipid Nanoparticles for Quercetin Brain Delivery and Alzheimer's Disease. *Pharm. Res.* **2020**, *37* (7), 139.
(23) Zhou, R.; Zhu, L.; Zeng, Z.; Luo, R.; Zhang, J.; Guo, R.; Zhang, L.; Zhang, Q.; Bi, W. Targeted Brain Delivery of RVG29-modified Rifampicin-loaded Nanoparticles for Alzheimer's Disease Treatment and Diagnosis. *Bioeng. Transl. Med.* **2022**, *7* (3), No. e10395.
(24) Lee, J. H.; Engler, J. A.; Collawn, J. F.; Moore, B. A. Receptor Mediated Uptake of Peptides That Bind the Human Transferrin Receptor. *Eur. J. Biochem.* **2001**, *268* (7), 2004−2012.
(25) Wang, Z.; Zhao, Y.; Jiang, Y.; Lv, W.; Wu, L.; Wang, B.; Lv, L.; Xu, Q.; Xin, H. Enhanced Anti-Ischemic Stroke of ZL006 by T7-Conjugated PEGylated Liposomes Drug Delivery System. *Sci. Rep.* **2015**, *5* (1), 12651.
(26) Bi, Y.; Liu, L.; Lu, Y.; Sun, T.; Shen, C.; Chen, X.; Chen, Q.; An, S.; He, X.; Ruan, C.; Wu, Y.; Zhang, Y.; Guo, Q.; Zheng, Z.; Liu, Y.; Lou, M.; Zhao, S.; Jiang, C. T7 Peptide-Functionalized PEG-PLGA Micelles Loaded with Carmustine for Targeting Therapy of Glioma. *ACS Appl. Mater. Interfaces* **2016**, *8* (41), 27465−27473.
(27) Kong, J.; Zou, R.; Law, G.-L.; Wang, Y. Biomimetic Multifunctional Persistent Luminescence Nanoprobes for Long-Term near-Infrared Imaging and Therapy of Cerebral and Cerebellar Gliomas. *Sci. Adv.* **2022**, *8* (10), No. eabm7077.
(28) Abe, E.; Fuwa, T. J.; Hoshi, K.; Saito, T.; Murakami, T.; Miyajima, M.; Ogawa, N.; Akatsu, H.; Hashizume, Y.; Hashimoto, Y.; Honda, T. Expression of Transferrin Protein and Messenger RNA in

https://doi.org/10.1021/acs.nanolett.4c05186
Nano Lett. 2025, 25, 800−810

Neural Cells from Mouse and Human Brain Tissue. *Metabolites* **2022**, *12* (7), 594.
(29) Demeule, M.; Régina, A.; Ché, C.; Poirier, J.; Nguyen, T.; Gabathuler, R.; Castaigne, J.-P.; Béliveau, R. Identification and Design of Peptides as a New Drug Delivery System for the Brain. *J. Pharmacol. Exp. Ther.* **2008**, *324* (3), 1064−1072.
(30) Demeule, M.; Currie, J.-C.; Bertrand, Y.; Ché, C.; Nguyen, T.; Régina, A.; Gabathuler, R.; Castaigne, J.-P.; Béliveau, R. Involvement of the Low-Density Lipoprotein Receptor-Related Protein in the Transcytosis of the Brain Delivery Vector Angiopep-2. *J. Neurochem.* **2008**, *106* (4), 1534−1544.
(31) Yuan, Z.; Zhao, L.; Zhang, Y.; Li, S.; Pan, B.; Hua, L.; Wang, Z.; Ye, C.; Lu, J.; Yu, R.; Liu, H. Inhibition of Glioma Growth by a GOLPH3 siRNA-Loaded Cationic Liposomes. *J. Neurooncol.* **2018**, *140* (2), 249−260.
(32) Israel, L. L.; Braubach, O.; Galstyan, A.; Chiechi, A.; Shatalova, E. S.; Grodzinski, Z.; Ding, H.; Black, K. L.; Ljubimova, J. Y.; Holler, E. A Combination of Tri-Leucine and Angiopep-2 Drives a Polyanionic Polymalic Acid Nanodrug Platform Across the Blood-Brain Barrier. *ACS Nano* **2019**, *13*, 1253.
(33) Shi, X.-X.; Miao, W.-M.; Pang, D.-W.; Wu, J.-S.; Tong, Q.-S.; Li, J.-X.; Luo, J.-Q.; Li, W.-Y.; Du, J.-Z.; Wang, J. Angiopep-2 Conjugated Nanoparticles Loaded with Doxorubicin for the Treatment of Primary Central Nervous System Lymphoma. *Biomater. Sci.* **2020**, *8* (5), 1290−1297.
(34) Hoyos-Ceballos, G. P.; Ruozi, B.; Ottonelli, I.; Da Ros, F.; Vandelli, M. A.; Forni, F.; Daini, E.; Vilella, A.; Zoli, M.; Tosi, G.; Duskey, J. T.; López-Osorio, B. L. PLGA-PEG-ANG-2 Nanoparticles for Blood-Brain Barrier Crossing: Proof-of-Concept Study. *Pharmaceutics* **2020**, *12* (1), 72.
(35) Costagliola di Polidoro, A.; Zambito, G.; Haeck, J.; Mezzanotte, L.; Lamfers, M.; Netti, P. A.; Torino, E. Theranostic Design of Angiopep-2 Conjugated Hyaluronic Acid Nanoparticles (Thera-ANG-cHANPs) for Dual Targeting and Boosted Imaging of Glioma Cells. *Cancers* **2021**, *13* (3), 503.
(36) Re, F.; Cambianica, I.; Zona, C.; Sesana, S.; Gregori, M.; Rigolio, R.; La Ferla, B.; Nicotra, F.; Forloni, G.; Cagnotto, A.; Salmona, M.; Masserini, M.; Sancini, G. Functionalization of Liposomes with ApoE-Derived Peptides at Different Density Affects Cellular Uptake and Drug Transport across a Blood-Brain Barrier Model. *Nanomedicine Nanotechnol. Biol. Med.* **2011**, *7* (5), 551−559.
(37) Dal Magro, R.; Ornaghi, F.; Cambianica, I.; Beretta, S.; Re, F.; Musicanti, C.; Rigolio, R.; Donzelli, E.; Canta, A.; Ballarini, E.; Cavaletti, G.; Gasco, P.; Sancini, G. ApoE-Modified Solid Lipid Nanoparticles: A Feasible Strategy to Cross the Blood-Brain Barrier. *J. Controlled Release* **2017**, *249*, 103−110.
(38) May, P.; Rohlmann, A.; Bock, H. H.; Zurhove, K.; Marth, J. D.; Schomburg, E. D.; Noebels, J. L.; Beffert, U.; Sweatt, J. D.; Weeber, E. J.; Herz, J. Neuronal LRP1 Functionally Associates with Postsynaptic Proteins and Is Required for Normal Motor Function in Mice. *Mol. Cell. Biol.* **2004**, *24* (20), 8872−8883.
(39) Schoenmaker, L.; Witzigmann, D.; Kulkarni, J. A.; Verbeke, R.; Kersten, G.; Jiskoot, W.; Crommelin, D. J. A. mRNA-Lipid Nanoparticle COVID-19 Vaccines: Structure and Stability. *Int. J. Pharm.* **2021**, *601*, 120586.
(40) Han, E. L.; Padilla, M. S.; Palanki, R.; Kim, D.; Mrksich, K.; Li, J. J.; Tang, S.; Yoon, I.-C.; Mitchell, M. J. Predictive High-Throughput Platform for Dual Screening of mRNA Lipid Nanoparticle Blood-Brain Barrier Transfection and Crossing. *Nano Lett.* **2024**, *24* (5), 1477−1486.
(41) Li, W.; Qiu, J.; Li, X.-L.; Aday, S.; Zhang, J.; Conley, G.; Xu, J.; Joseph, J.; Lan, H.; Langer, R.; Mannix, R.; Karp, J. M.; Joshi, N. BBB Pathophysiology-Independent Delivery of siRNA in Traumatic Brain Injury. *Sci. Adv.* **2021**, *7* (1), No. eabd6889.
(42) Monopoli, M. P.; Åberg, C.; Salvati, A.; Dawson, K. A. Biomolecular Coronas Provide the Biological Identity of Nanosized Materials. *Nat. Nanotechnol.* **2012**, *7* (12), 779−786.
(43) Chen, D.; Ganesh, S.; Wang, W.; Amiji, M. The Role of Surface Chemistry in Serum Protein Corona-Mediated Cellular Delivery and Gene Silencing with Lipid Nanoparticles. *Nanoscale* **2019**, *11* (18), 8760−8775.
(44) Xiao, W.; Wang, Y.; Zhang, H.; Liu, Y.; Xie, R.; He, X.; Zhou, Y.; Liang, L.; Gao, H. The Protein Corona Hampers the Transcytosis of Transferrin-Modified Nanoparticles through Blood-Brain Barrier and Attenuates Their Targeting Ability to Brain Tumor. *Biomaterials* **2021**, *274*, 120888.
(45) Salvati, A.; Pitek, A. S.; Monopoli, M. P.; Prapainop, K.; Bombelli, F. B.; Hristov, D. R.; Kelly, P. M.; Åberg, C.; Mahon, E.; Dawson, K. A. Transferrin-Functionalized Nanoparticles Lose Their Targeting Capabilities When a Biomolecule Corona Adsorbs on the Surface. *Nat. Nanotechnol.* **2013**, *8* (2), 137−143.
(46) Cox, A.; Andreozzi, P.; Dal Magro, R.; Fiordaliso, F.; Corbelli, A.; Talamini, L.; Chinello, C.; Raimondo, F.; Magni, F.; Tringali, M.; Krol, S.; Jacob Silva, P.; Stellacci, F.; Masserini, M.; Re, F. Evolution of Nanoparticle Protein Corona across the Blood-Brain Barrier. *ACS Nano* **2018**, *12* (7), 7292−7300.
(47) Paramasivam, P.; Franke, C.; Stöter, M.; Höijer, A.; Bartesaghi, S.; Sabirsh, A.; Lindfors, L.; Arteta, M. Y.; Dahlén, A.; Bak, A.; Andersson, S.; Kalaidzidis, Y.; Bickle, M.; Zerial, M. Endosomal Escape of Delivered mRNA from Endosomal Recycling Tubules Visualized at the Nanoscale. *J. Cell Biol.* **2022**, *221* (2), No. e202110137.
(48) Maugeri, M.; Nawaz, M.; Papadimitriou, A.; Angerfors, A.; Camponeschi, A.; Na, M.; Hölttä, M.; Skantze, P.; Johansson, S.; Sundqvist, M.; Lindquist, J.; Kjellman, T.; Mårtensson, I.-L.; Jin, T.; Sunnerhagen, P.; Östman, S.; Lindfors, L.; Valadi, H. Linkage between Endosomal Escape of LNP-mRNA and Loading into EVs for Transport to Other Cells. *Nat. Commun.* **2019**, *10* (1), 4333.
(49) Nawaz, M.; Heydarkhan-Hagvall, S.; Tangruksa, B.; González-King Garibotti, H.; Jing, Y.; Maugeri, M.; Kohl, F.; Hultin, L.; Reyahi, A.; Camponeschi, A.; Kull, B.; Christoffersson, J.; Grimsholm, O.; Jennbacken, K.; Sundqvist, M.; Wiseman, J.; Bidar, A. W.; Lindfors, L.; Synnergren, J.; Valadi, H. Lipid Nanoparticles Deliver the Therapeutic VEGFA mRNA In Vitro and In Vivo and Transform Extracellular Vesicles for Their Functional Extensions. *Adv. Sci.* **2023**, *10* (12), 2206187.
(50) Melamed, J. R.; Yerneni, S. S.; Arral, M. L.; LoPresti, S. T.; Chaudhary, N.; Sehrawat, A.; Muramatsu, H.; Alameh, M.-G.; Pardi, N.; Weissman, D.; Gittes, G. K.; Whitehead, K. A. Ionizable Lipid Nanoparticles Deliver mRNA to Pancreatic β Cells via Macrophage-Mediated Gene Transfer. *Sci. Adv.* **2023**, *9* (4), No. eade1444.
(51) Johnsen, K. B.; Burkhart, A.; Melander, F.; Kempen, P. J.; Vejlebo, J. B.; Siupka, P.; Nielsen, M. S.; Andresen, T. L.; Moos, T. Targeting Transferrin Receptors at the Blood-Brain Barrier Improves the Uptake of Immunoliposomes and Subsequent Cargo Transport into the Brain Parenchyma. *Sci. Rep.* **2017**, *7* (1), 10396.
(52) Akinc, A.; Querbes, W.; De, S.; Qin, J.; Frank-Kamenetsky, M.; Jayaprakash, K. N.; Jayaraman, M.; Rajeev, K. G.; Cantley, W. L.; Dorkin, J. R.; Butler, J. S.; Qin, L.; Racie, T.; Sprague, A.; Fava, E.; Zeigerer, A.; Hope, M. J.; Zerial, M.; Sah, D. W.; Fitzgerald, K.; Tracy, M. A.; Manoharan, M.; Koteliansky, V.; Fougerolles, A. de; Maier, M. A. Targeted Delivery of RNAi Therapeutics With Endogenous and Exogenous Ligand-Based Mechanisms. *Mol. Ther.* **2010**, *18* (7), 1357−1364.
(53) Sebastiani, F.; Yanez Arteta, M.; Lerche, M.; Porcar, L.; Lang, C.; Bragg, R. A.; Elmore, C. S.; Krishnamurthy, V. R.; Russell, R. A.; Darwish, T.; Pichler, H.; Waldie, S.; Moulin, M.; Haertlein, M.; Forsyth, V. T.; Lindfors, L.; Cárdenas, M. Apolipoprotein E Binding Drives Structural and Compositional Rearrangement of mRNA-Containing Lipid Nanoparticles. *ACS Nano* **2021**, *15* (4), 6709−6722.
(54) Dahlman, J. E.; Kauffman, K. J.; Xing, Y.; Shaw, T. E.; Mir, F. F.; Dlott, C. C.; Langer, R.; Anderson, D. G.; Wang, E. T. Barcoded Nanoparticles for High Throughput in Vivo Discovery of Targeted Therapeutics. *Proc. Natl. Acad. Sci. U. S. A.* **2017**, *114* (8), 2060−2065.
(55) Guimaraes, P. P.; Zhang, R.; Spektor, R.; Tan, M.; Chung, A.; Billingsley, M. M.; El-Mayta, R.; Riley, R. S.; Wang, L.; Wilson, J. M.;

https://doi.org/10.1021/acs.nanolett.4c05186
Nano Lett. 2025, 25, 800−810

Mitchell, M. J. Ionizable Lipid Nanoparticles Encapsulating Barcoded mRNA for Accelerated in Vivo Delivery Screening. *J. Control. Release Off. J. Control. Release Soc.* **2019**, *316*, 404−417.
(56) Rhym, L. H.; Manan, R. S.; Koller, A.; Stephanie, G.; Anderson, D. G. Peptide-Encoding mRNA Barcodes for the High-Throughput in Vivo Screening of Libraries of Lipid Nanoparticles for mRNA Delivery. *Nat. Biomed. Eng.* **2023**, *7* (7), 901−910.
(57) Hamilton, A. G.; Swingle, K. L.; Thatte, A. S.; Mukalel, A. J.; Safford, H. C.; Billingsley, M. M.; El-Mayta, R. D.; Han, X.; Nachod, B. E.; Joseph, R. A.; Metzloff, A. E.; Mitchell, M. J. High-Throughput In Vivo Screening Identifies Differential Influences on mRNA Lipid Nanoparticle Immune Cell Delivery by Administration Route. *ACS Nano* **2024**, *18* (25), 16151−16165.
(58) Han, L.; Jiang, C. Evolution of Blood-Brain Barrier in Brain Diseases and Related Systemic Nanoscale Brain-Targeting Drug Delivery Strategies. *Acta Pharm. Sin. B* **2021**, *11* (8), 2306−2325.
(59) Islam, Y.; Leach, A. G.; Smith, J.; Pluchino, S.; Coxon, C. R.; Sivakumaran, M.; Downing, J.; Fatokun, A. A.; Teixidò, M.; Ehtezazi, T. Physiological and Pathological Factors Affecting Drug Delivery to the Brain by Nanoparticles. *Adv. Sci.* **2021**, *8* (11), 2002085.
(60) Shibata, M.; Yamada, S.; Kumar, S. R.; Calero, M.; Bading, J.; Frangione, B.; Holtzman, D. M.; Miller, C. A.; Strickland, D. K.; Ghiso, J.; Zlokovic, B. V. Clearance of Alzheimer's Amyloid-B1−40 Peptide from Brain by LDL Receptor-Related Protein-1 at the Blood-Brain Barrier. *J. Clin. Invest.* **2000**, *106* (12), 1489−1499.

https://doi.org/10.1021/acs.nanolett.4c05186
Nano Lett. 2025, 25, 800−810